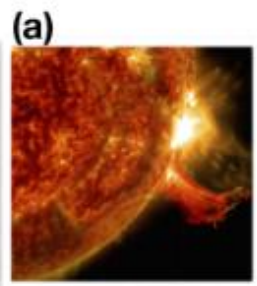# 磁重联中的KAW与高能电子

董全力

HITWH，20240729
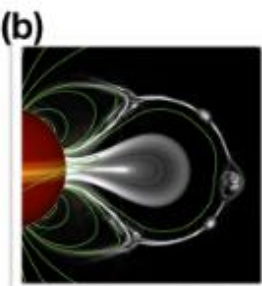
磁重联普遍发生在各种等离子体系统
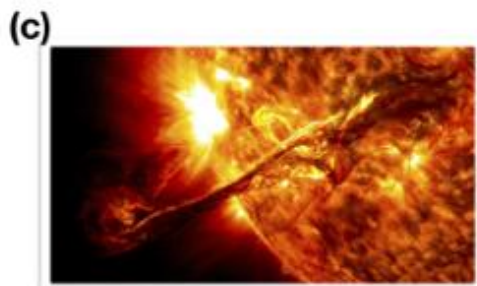

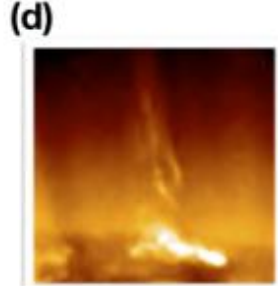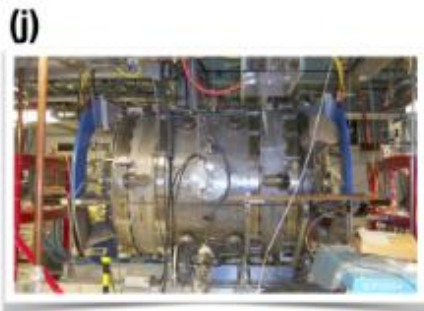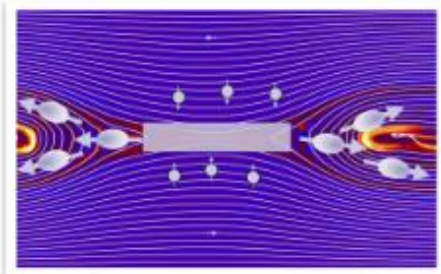Some Settings Where Reconnection Occurs

(a) Solar flares
(b) CMEs
(c) Prominence Eruptions
(d) Coronal Jets
(j) Laboratory Experiments/Fusion
(e) Earth's Magnetosphere
(i) X-ray Flares in Pulsar Wind Nebulae
(h) Active Galactic Nuclei Jets
(g) Edge of Heliosphere
(f) Planetary Magnetospheres
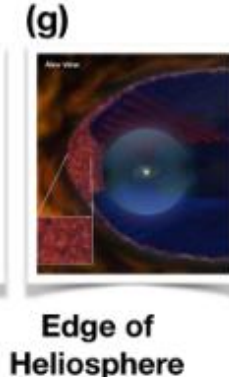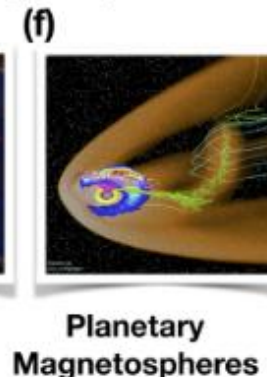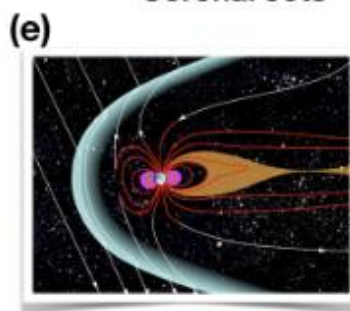
（1）等离子体参数范围广；
（2）物理过程空间尺度范围大；
（3）易发生；
（4）各种测量研究手段各有局限性；
（5）激光等离子体磁重联实验优势：
　条件可控；
　全局全过程；
　信号强；
　探测设备时空分辨率高；
　……

M. Hesse and P.A. Cassak, Magnetic Reconnection in the Space Sciences: Past, Present, and Future, Journal of Geophysical Research: Space Physics 125, （2020)

磁重联的Hall结构：观测与实验的测量对象
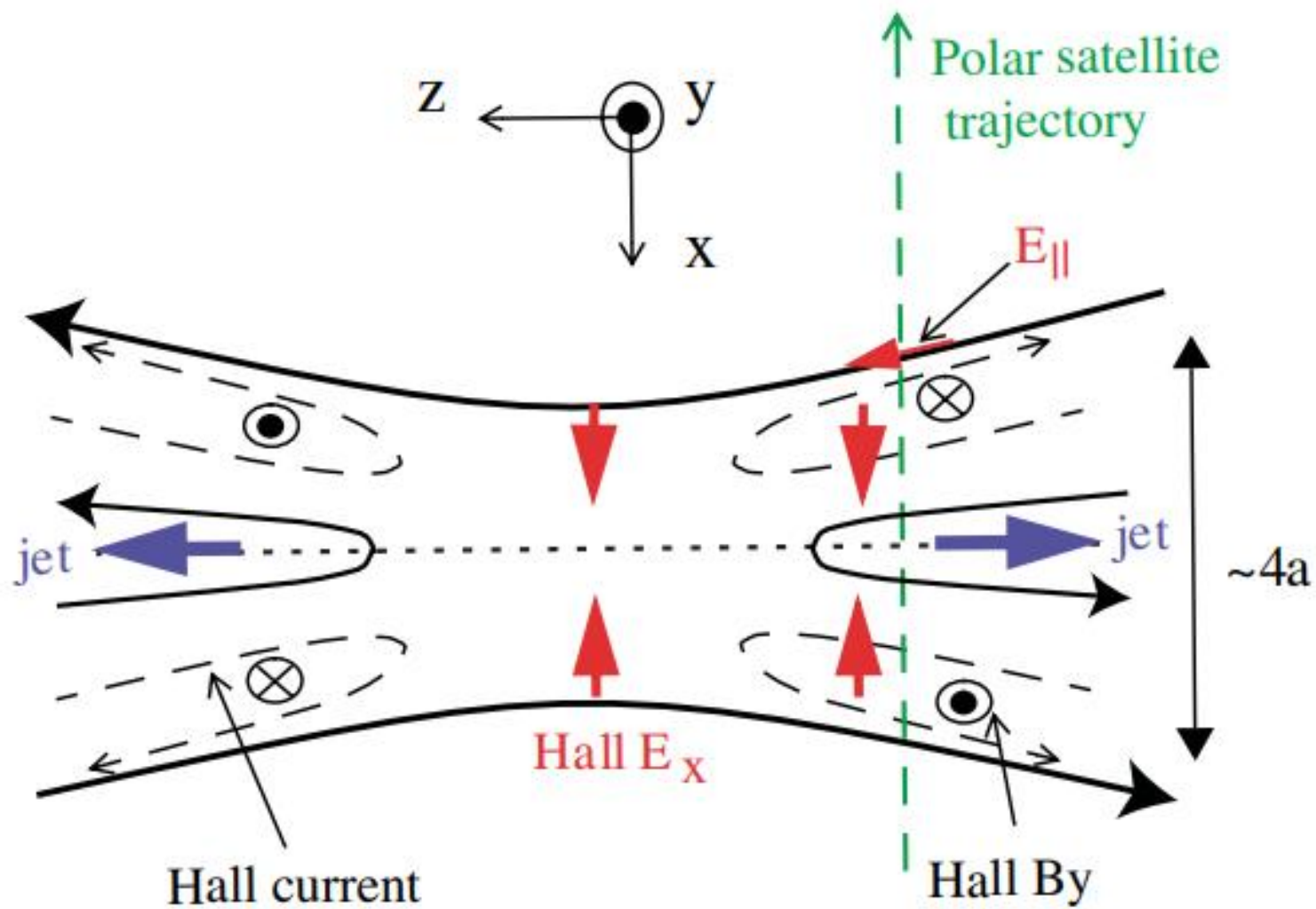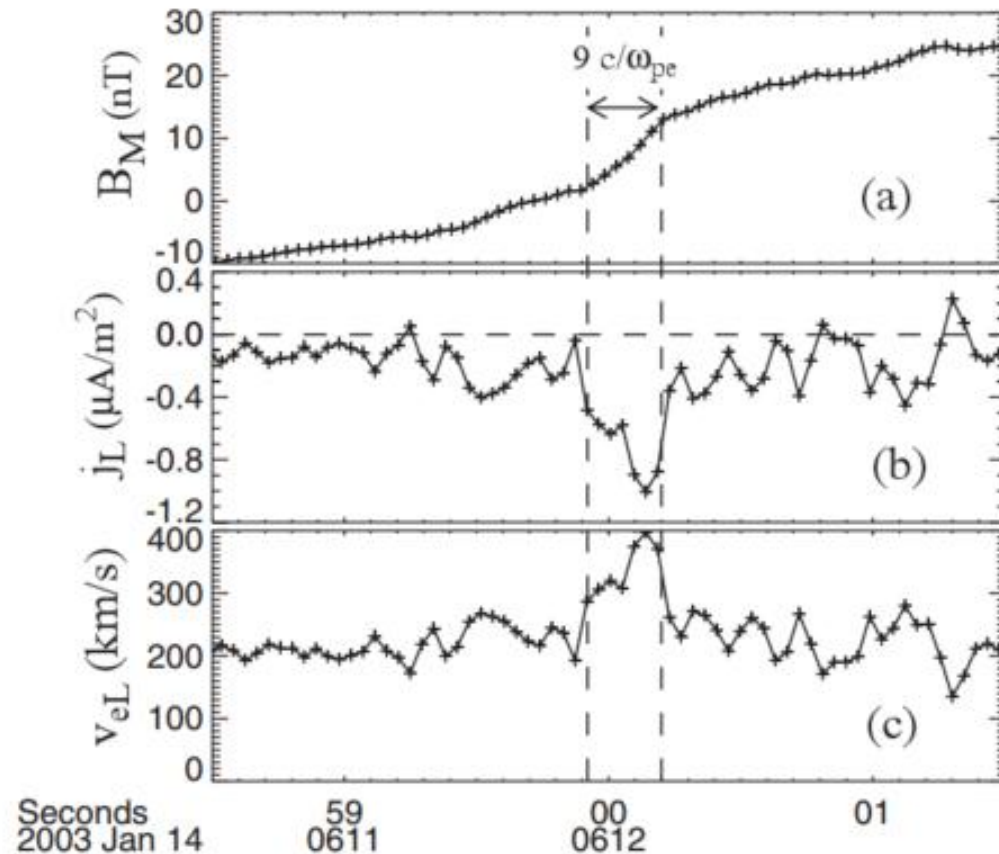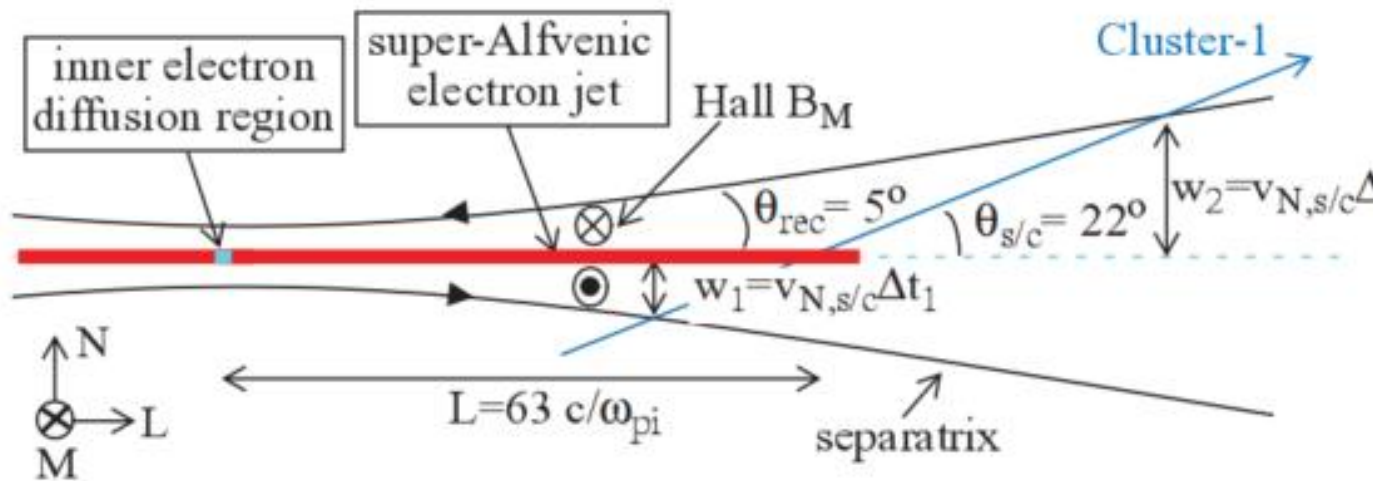
T.D. Phan, J.F. Drake, M.A. Shay, F.S. Mozer, and J.P. Eastwood, Evidence for an elongated (>60 ion skin depths) electron diffusion region during fast magnetic reconnection, Phys. Rev. Lett. 99, 255002 (2007).

当事件发生时，卫星必须在这个位置
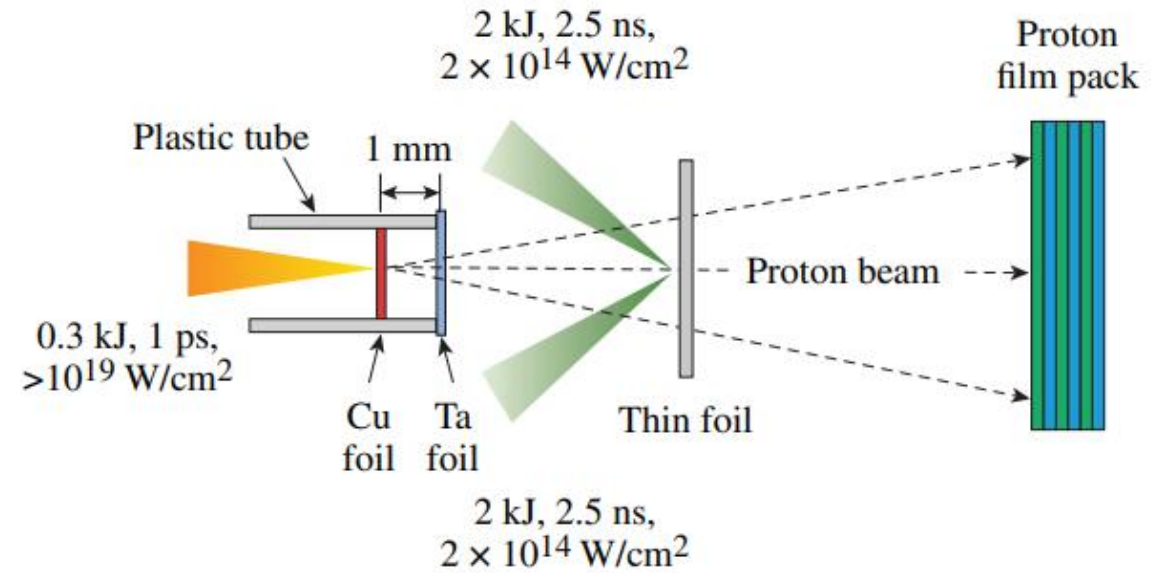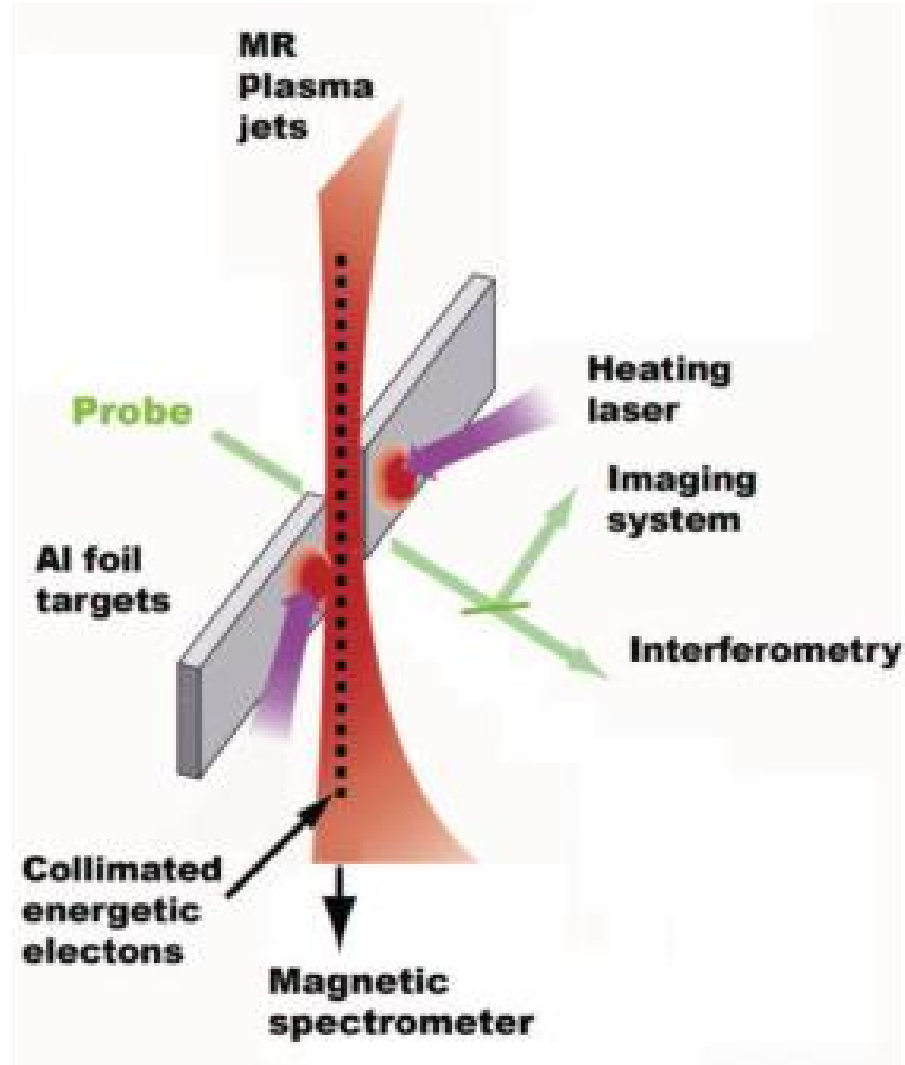
激光等离子体磁重联实验丰富的诊断手段
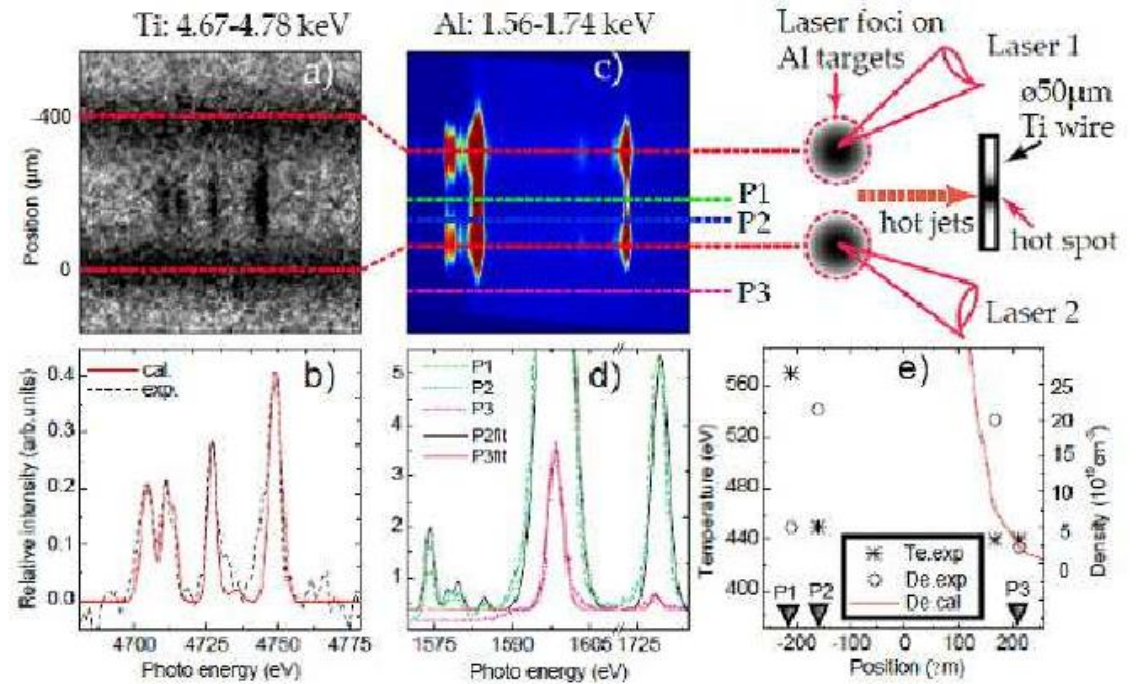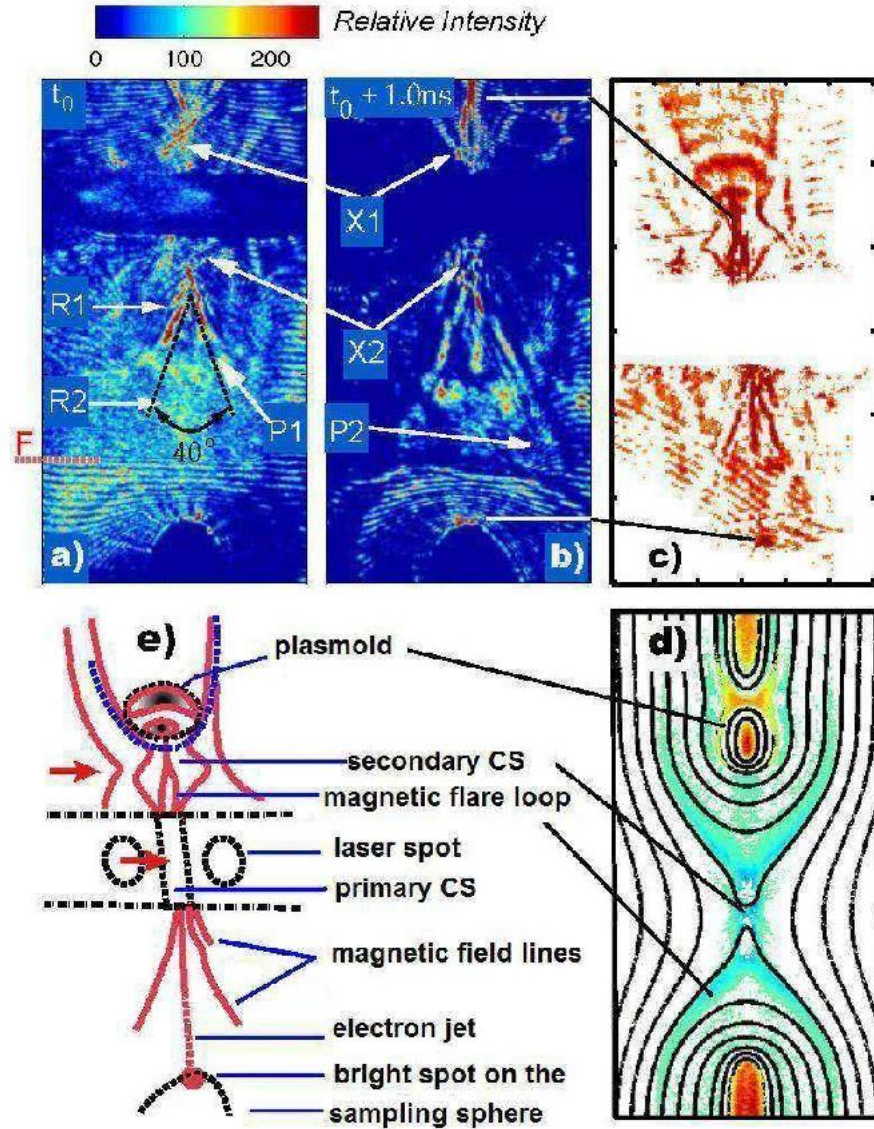
LP磁重联区中心高能电子束： MIT质子磁场观测
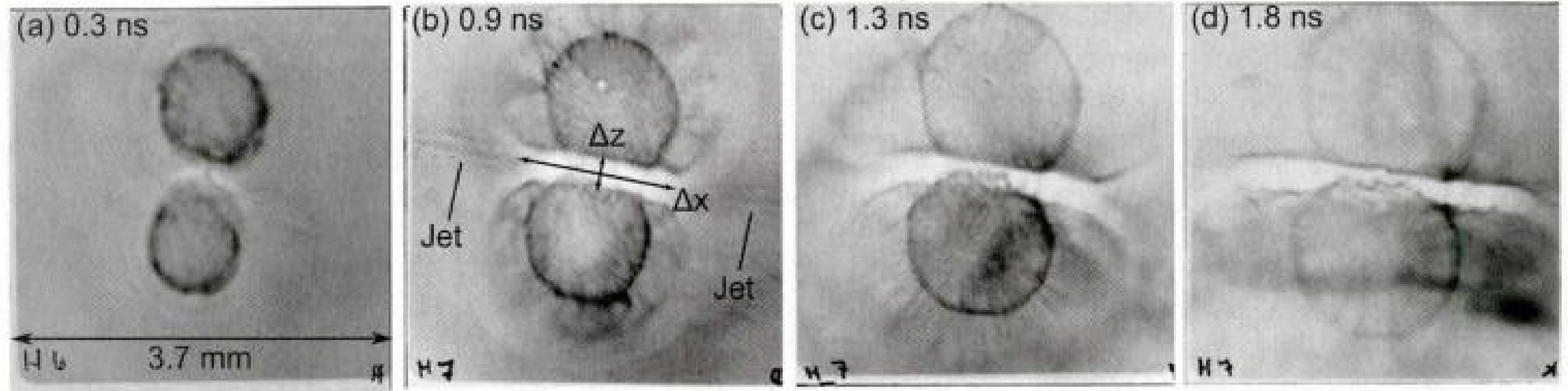
(a) 0.3 ns — 3.7 mm

(b) 0.9 ns — Δz, Δx, Jet, Jet

(c) 1.3 ns

(d) 1.8 ns

M.J. Rosenberg et al. Slowing of Magnetic Reconnection Concurrent with Weakening Plasma Inflows……. Phys. Rev. Lett. 114, 205004 (2015).

(a) $t_0 + 0.17$ ns

(b) $t_0 + 0.27$ ns

(c) $t_0 + 0.37$ ns

(d) $t_0 + 0.47$ ns

(e) $t_0 + 0.67$ ns

(f) $t_0 + 1.17$ ns

(g) $t_0 + 1.47$ ns

(h) $t_0 + 1.97$ ns
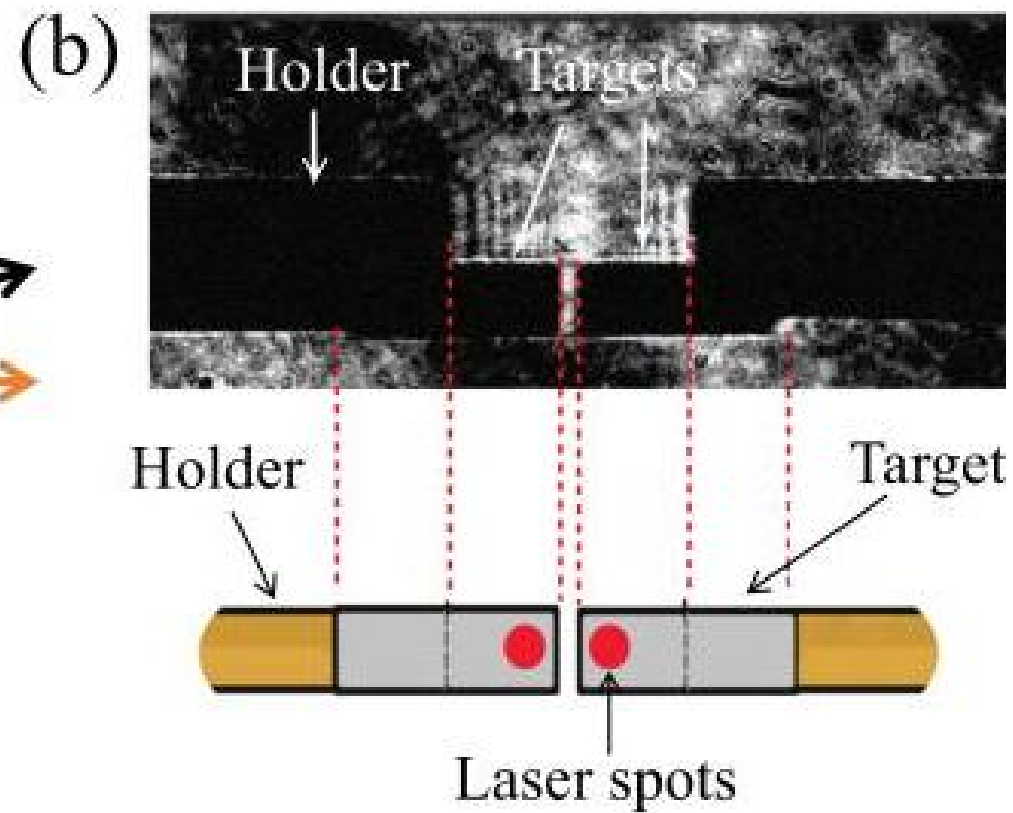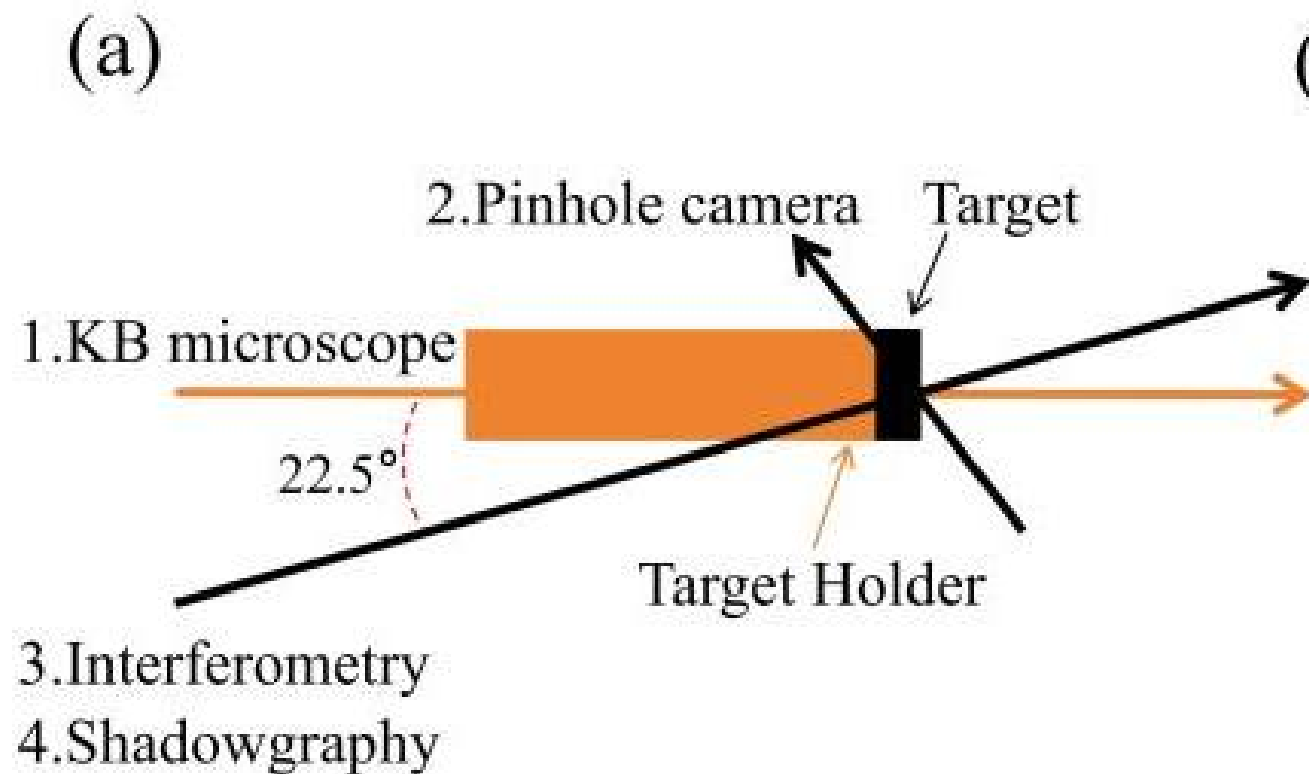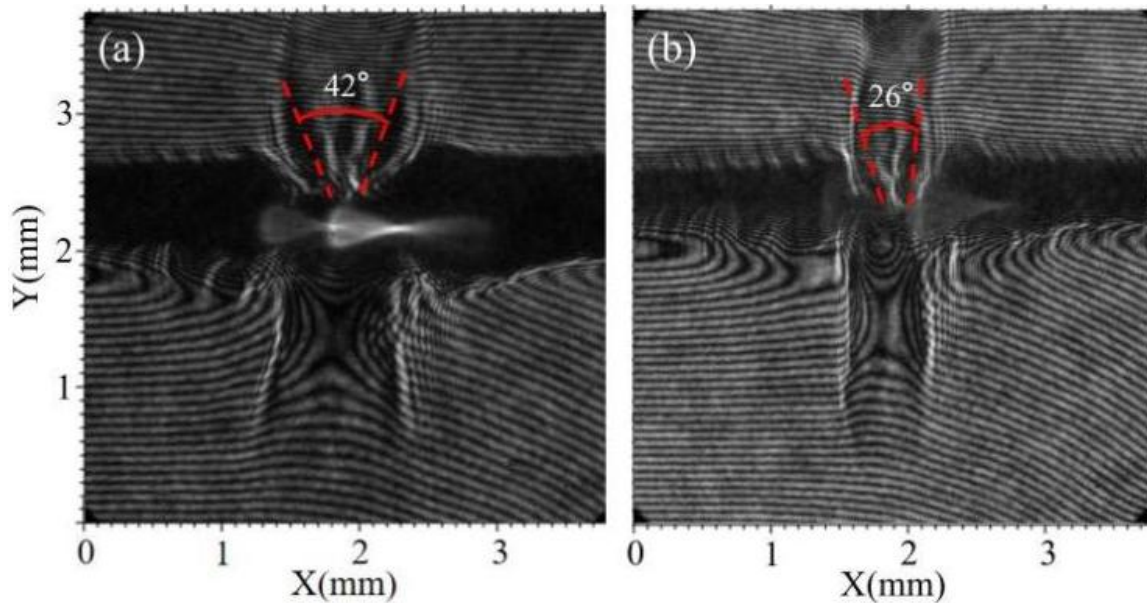
(a)激光焦斑相距350μm (b)600μm
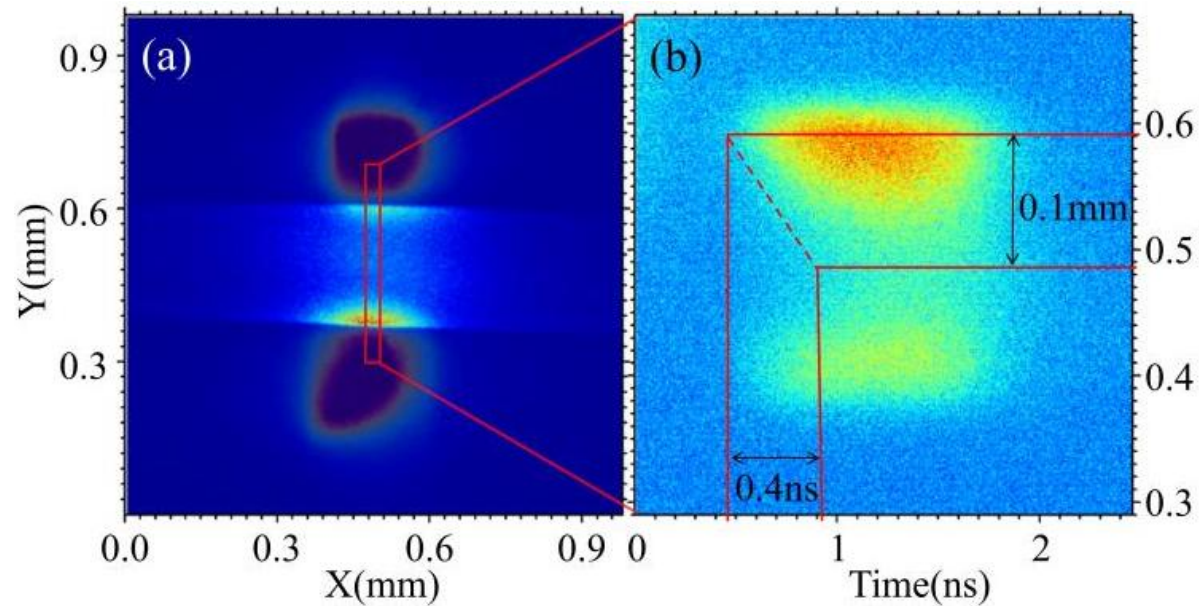
$$\text{v}_p \sim 250\text{km}/\text{s}$$
$$\text{v}_p = 3c_s$$
$$c_s = \sqrt{k_B T / m_i}$$
$$T \sim 590\text{eV}$$
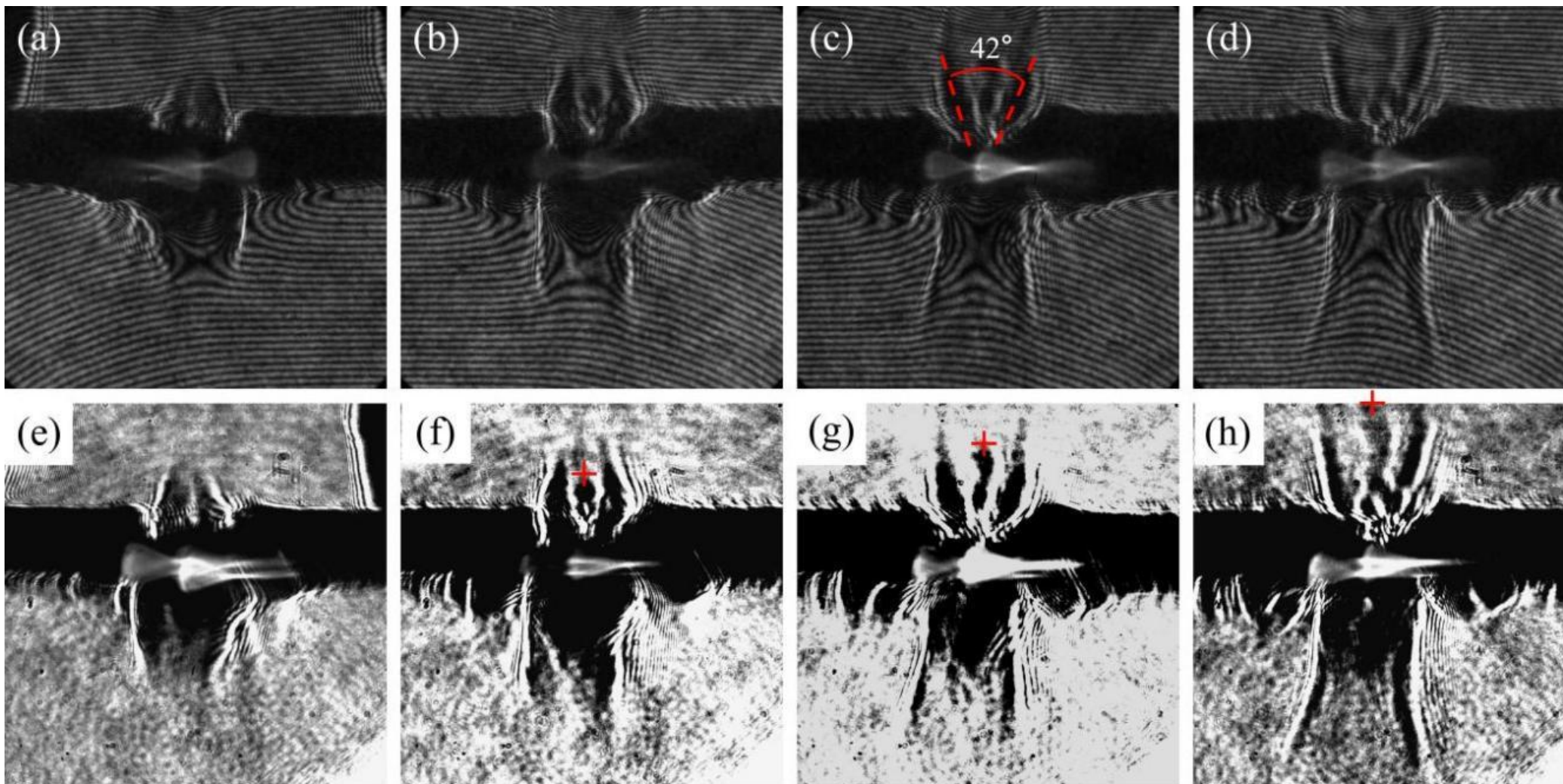
激光焦斑相距350 μm时等离子体演化
(a)-(d)干涉成像 (e)-(f)阴影成像

激光等离子体驱动磁重联：origin of jets
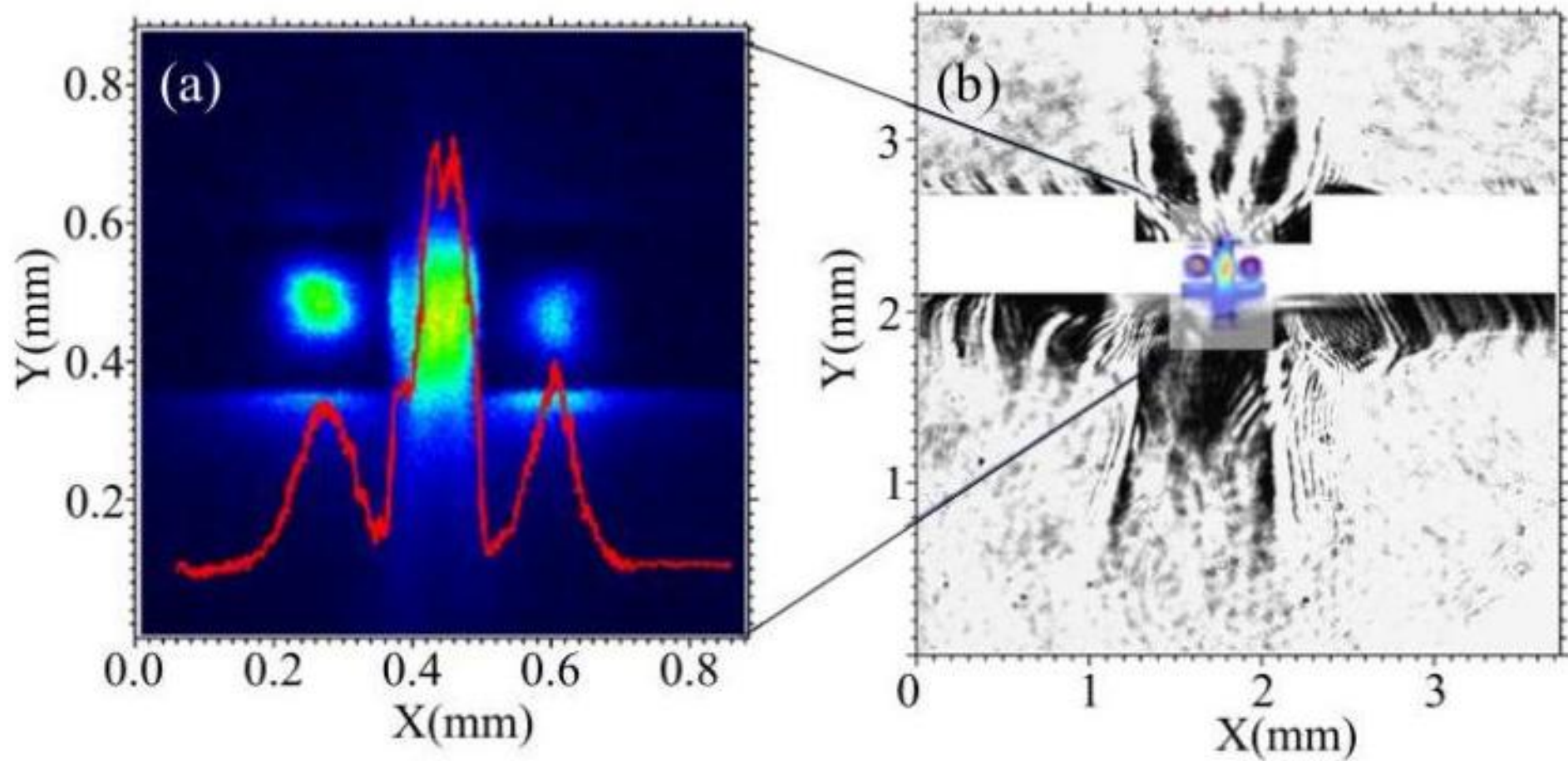
激光等离子体驱动磁重联：R ∝ opening angle

$$\frac{B_{xm}}{B_{x0}} \simeq \frac{1 - (\Delta z / \Delta x)^2}{1 + (\Delta z / \Delta x)^2}.$$

$$V_{out,m} \simeq c\sqrt{\frac{(1 - \delta^2/L^2)\sigma_{xm}}{1 + (1 - \delta^2/L^2)\sigma_{xm}}}$$

$$R_0 \simeq \left(\frac{B_{zm}}{B_{xm}}\right)\left(\frac{B_{xm}}{B_{x0}}\right)\left(\frac{V_{out,m}}{V_{A0}}\right)$$

$$R_{0,NR} \simeq \frac{\Delta z}{\Delta x}\left(\frac{1 - (\Delta z / \Delta x)^2}{1 + (\Delta z / \Delta x)^2}\right)^2 \sqrt{1 - \left(\frac{\Delta z}{\Delta x}\right)^2}$$

(a)激光焦斑相距350μm (b)600μm

$$R \sim 0.26$$

Y. Liu, M. Hesse, F. Guo, W. Daughton, H. Li, P.A. Cassak, and M.A. Shay, Why does steady-state magnetic reconnection have a maximum local rate of order 0.1? Phys. Rev. Lett. 118, 85101 (2017).
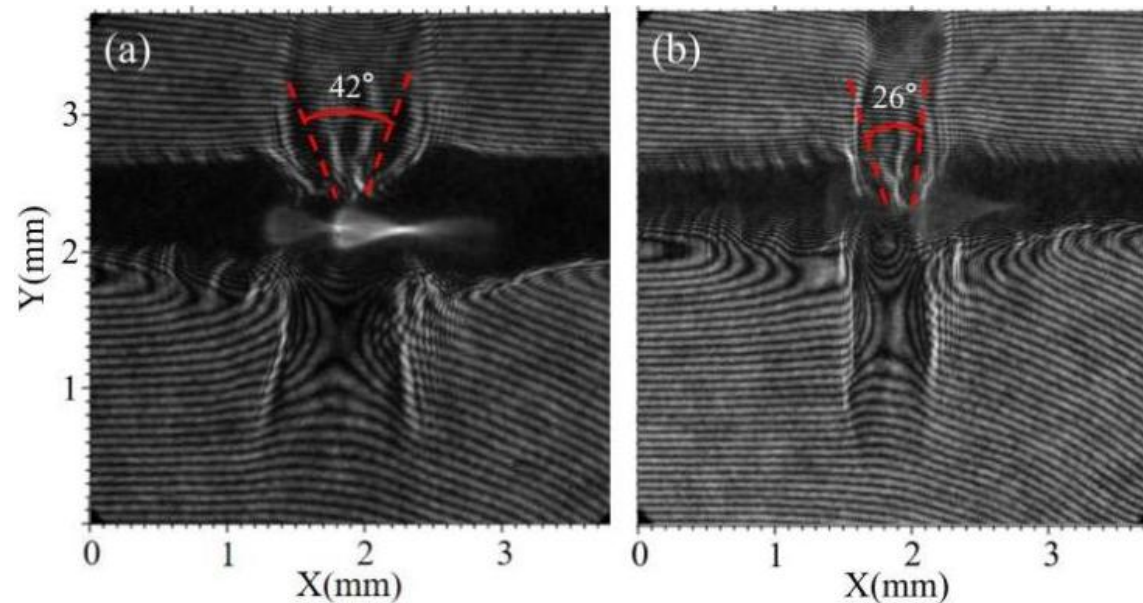
激光等离子体驱动磁重联中的KAW

MHD表面波与KAW的耦合方程

$$\left(\frac{\omega^2}{k_z^2 v_A^2} \frac{3}{4} \rho_i^2 \frac{d^3}{dx^3} + \frac{d^2}{dx^2} \frac{1}{g} \frac{T_e}{T_i} \rho_i^2 \frac{d}{dx} \right) \left(g \frac{d\Phi}{dx} \right) + \left[\frac{d}{dx} \left(\frac{\omega^2}{k_z^2 v_A^2} g - 1 \right) \frac{d}{dx} - k_y^2 \left(\frac{\omega^2}{k_z^2 v_A^2} - 1 \right) \right] \Phi = 0$$

波动方程可以化简为 $\qquad \rho^2 \frac{d^2 E_x}{dx^2} + \kappa x E_x = E_0$

仅考虑KAW向高密度侧传播，得到x方向上的波电场为 $\qquad E_{xnc} = \dfrac{v_A}{\left(\kappa \bar{\rho} \right)^{1/2}} B_{sy}$

KAW的极化关系满足 $\qquad E_{\parallel} = \rho_i^2 \dfrac{T_e}{T_i} \dfrac{\partial}{\partial z} \left(\nabla \cdot \delta E_{\perp} \right)$

此时KAW携带的平行电场为 $\qquad E_{\parallel nc} = i k_z \dfrac{T_e}{T_i} \left(k_x \rho_i \right)^2 \dfrac{v_A}{k_x} \dfrac{B_{sy}}{\left(\kappa \rho_i \right)^{1/2}}$
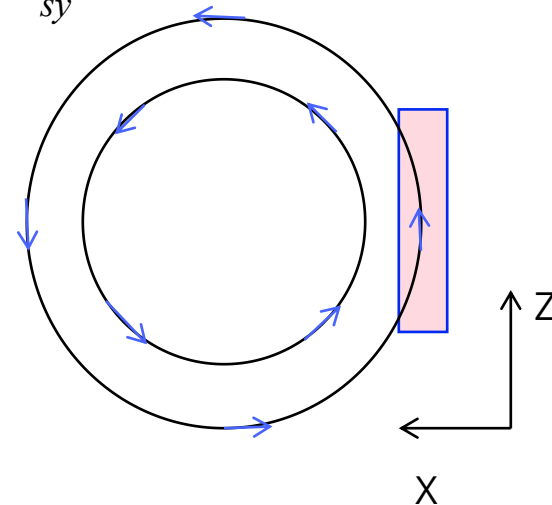
压缩波在在阿尔芬场线共振点与KAWs耦合

$$k_{\parallel}^2 v_A^2 (1+\Delta)\rho_i^2 \frac{d^4\Phi}{dx^4} + \frac{d}{dx}(\omega^2 - k_{\parallel}^2 v_A^2)\frac{d\Phi}{dx} + (\omega^2 - k_{\parallel}^2 v_A^2)(\omega^2 - k_y^2 v_A^2 - k_{\parallel}^2 v_A^2)\Phi / v_A^2 = 0$$

KAW x方向的电场分量为：

$$E_{xc} = (\frac{\omega}{k_y} B_{cz} + v_A B_{cy})(\kappa\bar{\rho})^{-1/2} + \frac{\gamma_e k_B \nabla n_1}{en_0}$$

由极化关系得到此时KAW的平行电场为：

$$E_{\parallel c} = (k_z^3 \frac{1}{k_y} B_z + k_z k_x B_y)\rho_i^2 \frac{T_e}{T_i} \frac{v_A}{(\kappa\bar{\rho})^{1/2}} + \frac{T_e}{T_i} k_x k_z \frac{\gamma_e k_B \nabla n_1}{en_0} \qquad (2)$$
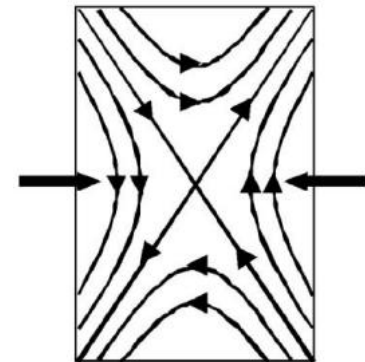
激光等离子体驱动磁重联中的KAW

参数:

(1) $\lambda_{//}$=100 μm，对于KAW，$k_{\perp}$>>$k_{//}$，取$k_{\perp}$=100$k_{//}$。

(2) n_{e0}~5×10²⁰ cm⁻³，平均离子电荷约为Z~10，离子密度为n_{i0}~5×10¹⁹ cm⁻³。

(3) $T_e = 110 \times a_0^{1.26}$ ，实验中激光强度为5×10¹⁵ W/cm²，T_e~790 eV。

(4) $\partial \mathbf{B}/\partial t \propto \nabla T_e \times \nabla n_e \sim 2MG$

KAW的平行电场 $E_{\|nc} = ik_z \frac{T_e}{T_i}\left(k_x\rho_i\right)^2 \frac{v_A}{k_x}\frac{B_{sy}}{\left(\kappa\rho_i\right)^{1/2}}$

$$E_{\|c} = (k_z^{\ 3}\frac{1}{k_y}B_z + k_z k_x B_y)\rho_i^2 \frac{T_e}{T_i}\frac{v_A}{\left(\kappa\bar{\rho}\right)^{1/2}} + \frac{T_e}{T_i}k_x k_z \frac{\gamma_e k_B \nabla n_1}{en_0}$$

平行电场可将电子加速到MeV量级

快速磁重联率
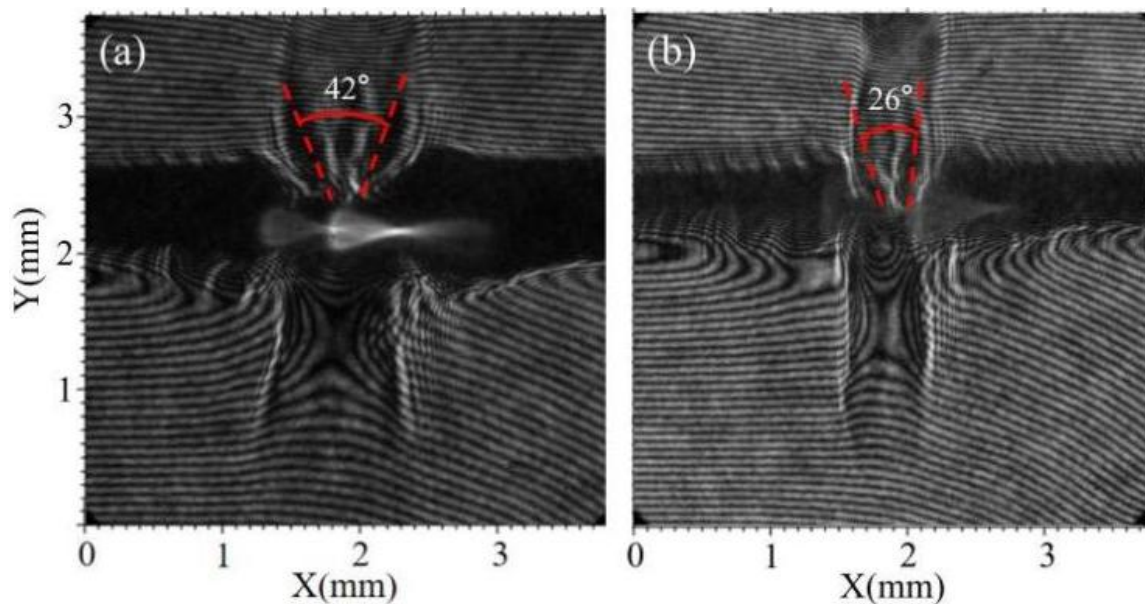
(a)激光焦斑相距350μm (b)600μm

$R \sim 0.26$

$$E_y \propto \left(n_1/n_e\right) v_{ex} v_{ey}, R = E_y \Big/ v_A B_y$$

$E_y \sim 7 \times 10^8$ V/m

$R \sim 0.3$

W. Wan and G. Lapenta, Electron self-reinforcing process of magnetic reconnection, Phys. Rev. Lett. 101, 15001 (2008).

由高能电子估计的重联率与opening angle估计的重联率一致

结论：KAW对电子的加速是LPMR的起因

（1）相对运动的等离子体引起对方磁场扰动进而产生KAWs加速电子形成出流区边界；
（2）等离子体进一步膨胀、碰撞、挤压，在中间区域形成双"Y"型结构；
（3）被压缩的呈长条状分布的磁场仍携带有KAW的平行电场，加速电子；
　　且重联磁场尚不足以偏转该部分电子，形成中间电子束；
（4）磁重联继续进行；

结论：KAW对电子的加速是LPMR的起因

（1）相对运动的等离子体引起对方磁场扰动进而产生KAWs加速电子形成出流区边界；
（2）等离子体进一步膨胀、碰撞、挤压，在中间区域形成双"Y"型结构；
（3）被压缩的呈长条状分布的磁场仍携带有KAW的平行电场，加速电子；
　　　且重联磁场尚不足以偏转该部分电子，形成中间电子束；
（4）磁重联继续进行；

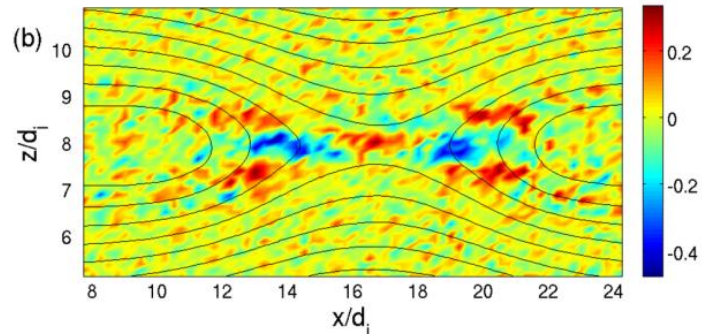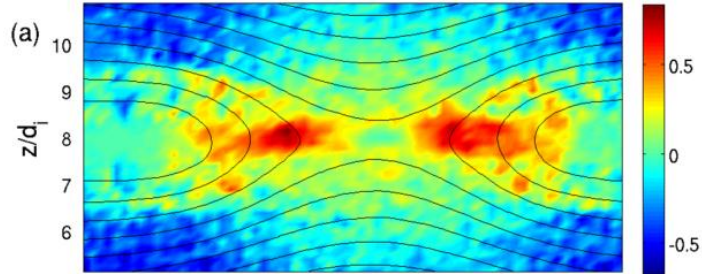## 感谢大家！

■电子加速机制

■磁重联与KAW

■激光等离子体驱动磁重联实验

■激光等离子体驱动磁重联中的KAW

电子加速机制

• **重联电场加速**

$$E = -V_i \times B + \frac{1}{ne} j \times B - \frac{m_e}{e} \frac{dV_e}{dt} - \frac{1}{ne} \nabla \cdot \vec{P}^{(e)}$$

$$E_y = -\left(V_{iz}B_x - V_{ix}B_z\right) + \frac{1}{ne}\left(j_z B_x - j_x B_z\right)$$

$$-\frac{m_e}{e}\left(\frac{\partial V_{ey}}{\partial t} + V_{ex}\frac{\partial V_{ey}}{\partial x} + V_{ez}\frac{\partial V_{ey}}{\partial z}\right) - \frac{1}{ne}\left(\frac{\partial P_{xy}^{(e)}}{\partial x} + \frac{\partial P_{zy}^{(e)}}{\partial z}\right)$$
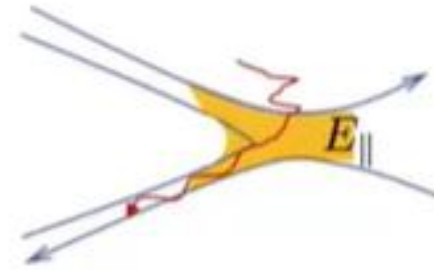

$$E_y\left(P_{exy}\right) \propto \frac{n_1}{n_e}\Delta u_y \Delta u_x$$
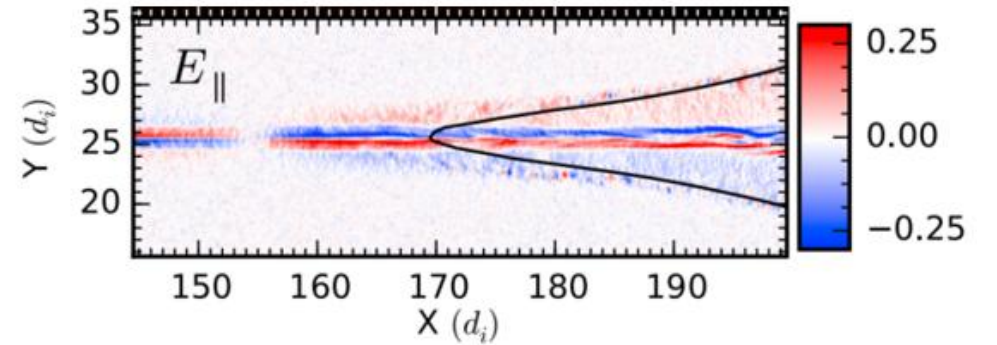
$$d\Delta u_y / dt = -eE_y / m_e$$

(a) 对流项和Hall项(b)电子压强张量项

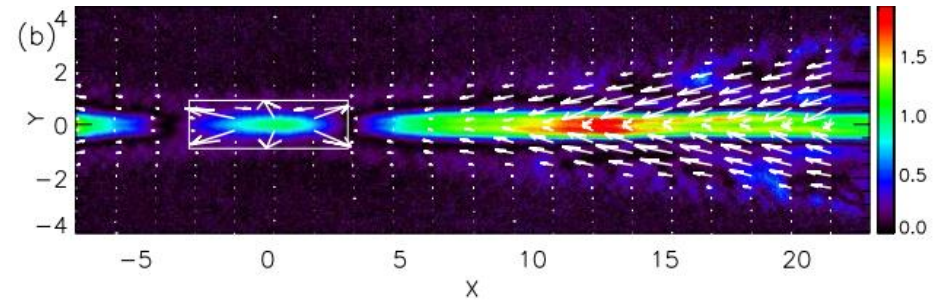W. Wan and G. Lapenta, Electron self-reinforcing process of magnetic reconnection, Phys. Rev. Lett. 101, 15001 (2008).

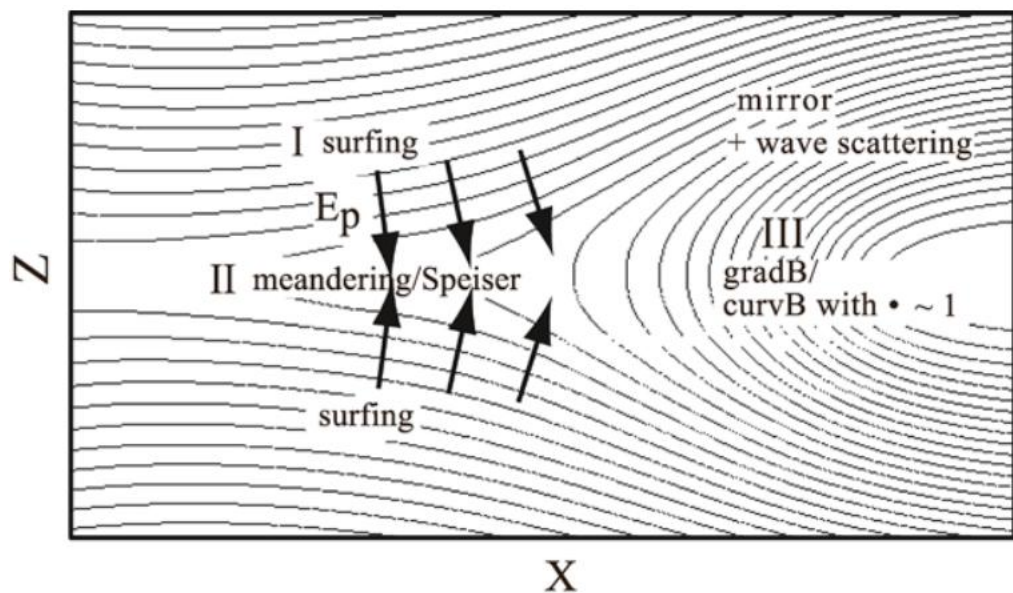$$\frac{d\varepsilon}{dt} = q\mathbf{E}_{\parallel} \cdot \mathbf{v}_{\parallel}$$

C.C. Haggerty, M.A. Shay, J.F. Drake, T.D. Phan, and C.T. McHugh, The competition of electron and ion heating during magnetic reconnection, （2015).

M.A. Shay, J.F. Drake, and M. Swisdak, Two-scale structure of the electron dissipation region during collisionless magnetic reconnection, Phys. Rev. Lett. 99, 155002 (2007).
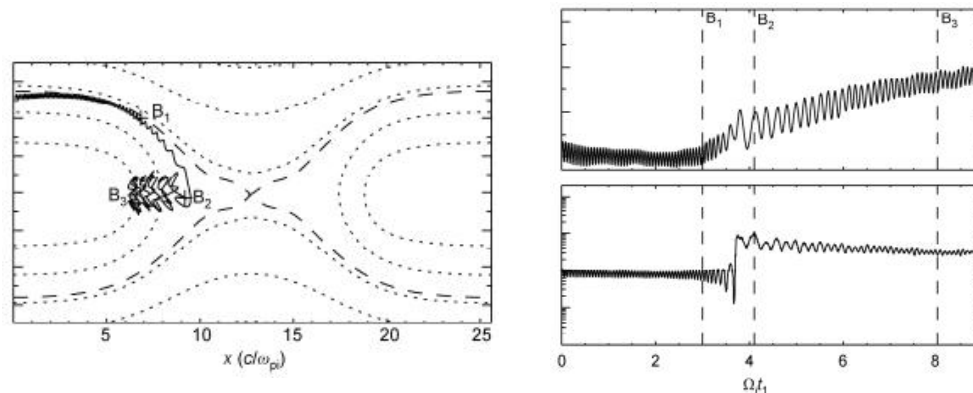
电子加速机制

M. Hoshino, Electron surfing acceleration in magnetic reconnection, J. Geophys Res. 110, (2005).
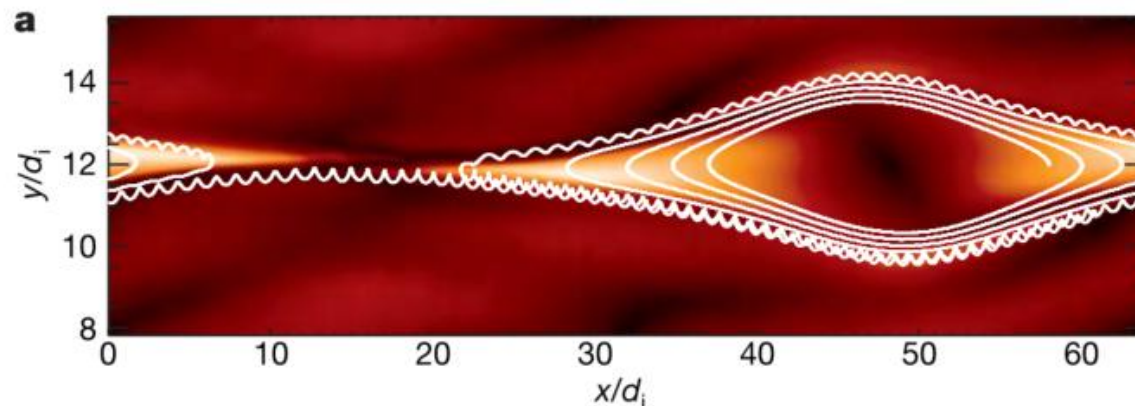
多阶段加速模型：

1. the Speiser motion in the diffusion region

2. the chaotic, gradient/curvature B drift motion in the magnetic field pileup region

3. the surfing/surfatron acceleration in the boundary

- **磁力线堆积区非绝热加速**

C. Huang, Q. Lu, and S. Wang, The mechanisms of electron acceleration in antiparallel and guide field magnetic reconnection, Phys. Plasmas 17, 72306 (2010).

- **磁岛加速**

J.F. Drake, M. Swisdak, H. Che, and M.A. Shay, Electron acceleration from contracting magnetic islands during reconnection, Nature 443, 553-556 (2006).

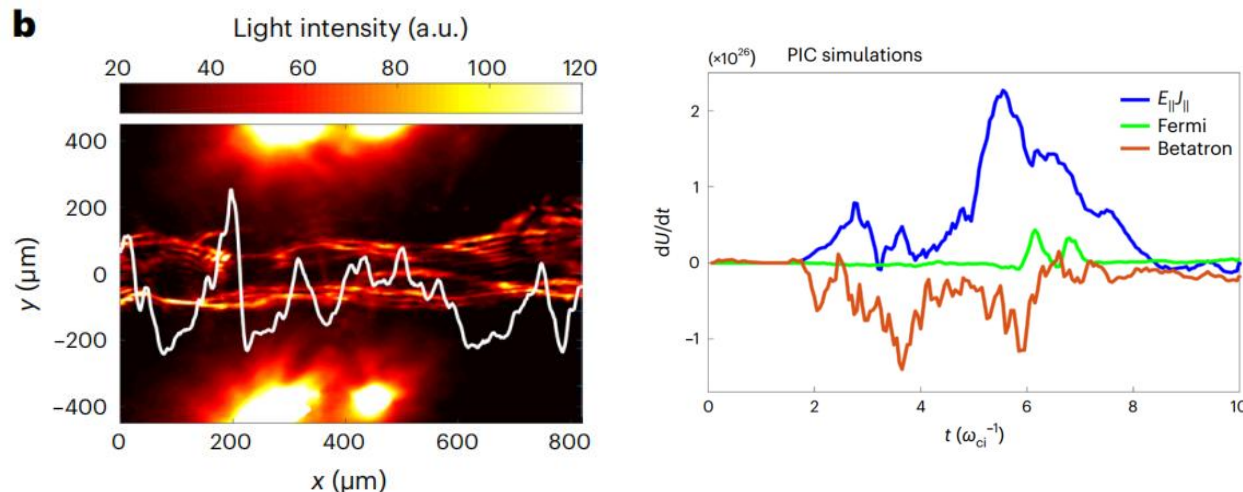反射一次获得的能量增益 $\dfrac{d\varepsilon_{\parallel}}{dt} = -2\varepsilon_{\parallel}\dfrac{u_x}{\delta_x}\dfrac{B_x^2}{B^2}$

磁岛长度变化带来的总能量变化 $\mathrm{d}W = 2\dfrac{d\delta_x}{\delta_x}\dfrac{B_x^2}{8\pi}\left(1 - \dfrac{8\pi\overline{\varepsilon_{\parallel}}}{B^2}\right)$
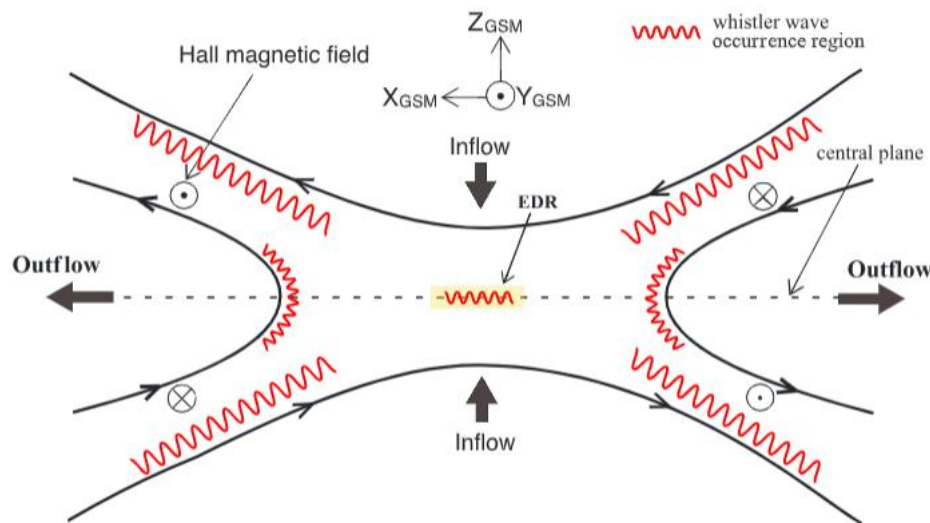
电子加速机制

- **湍流和波**
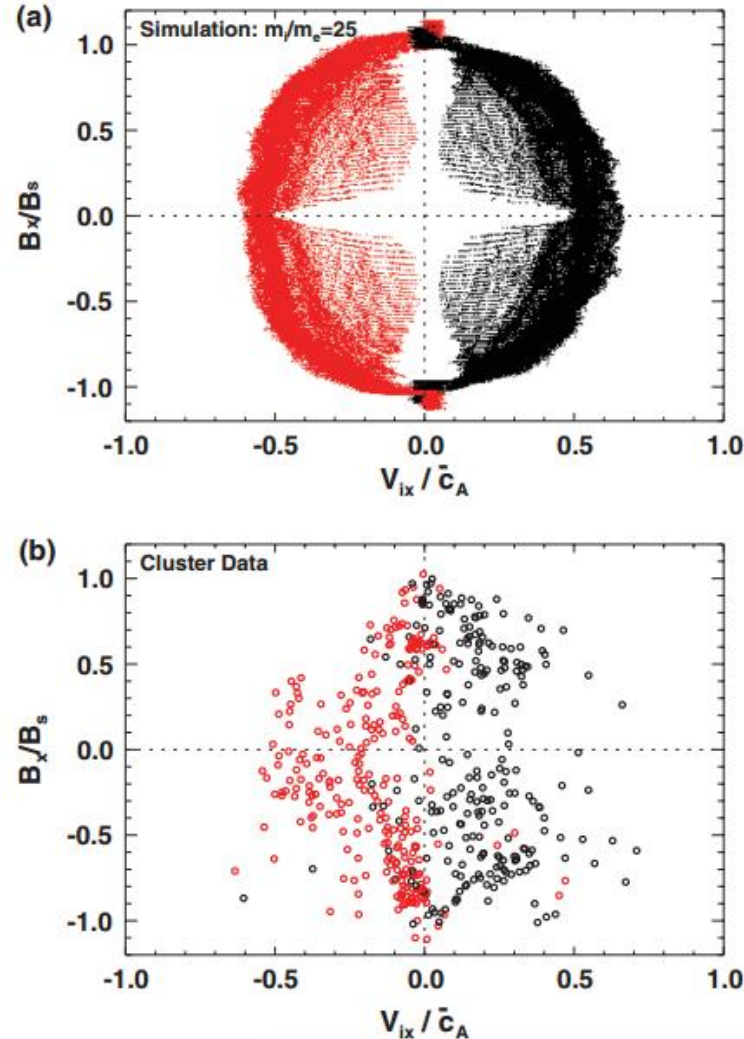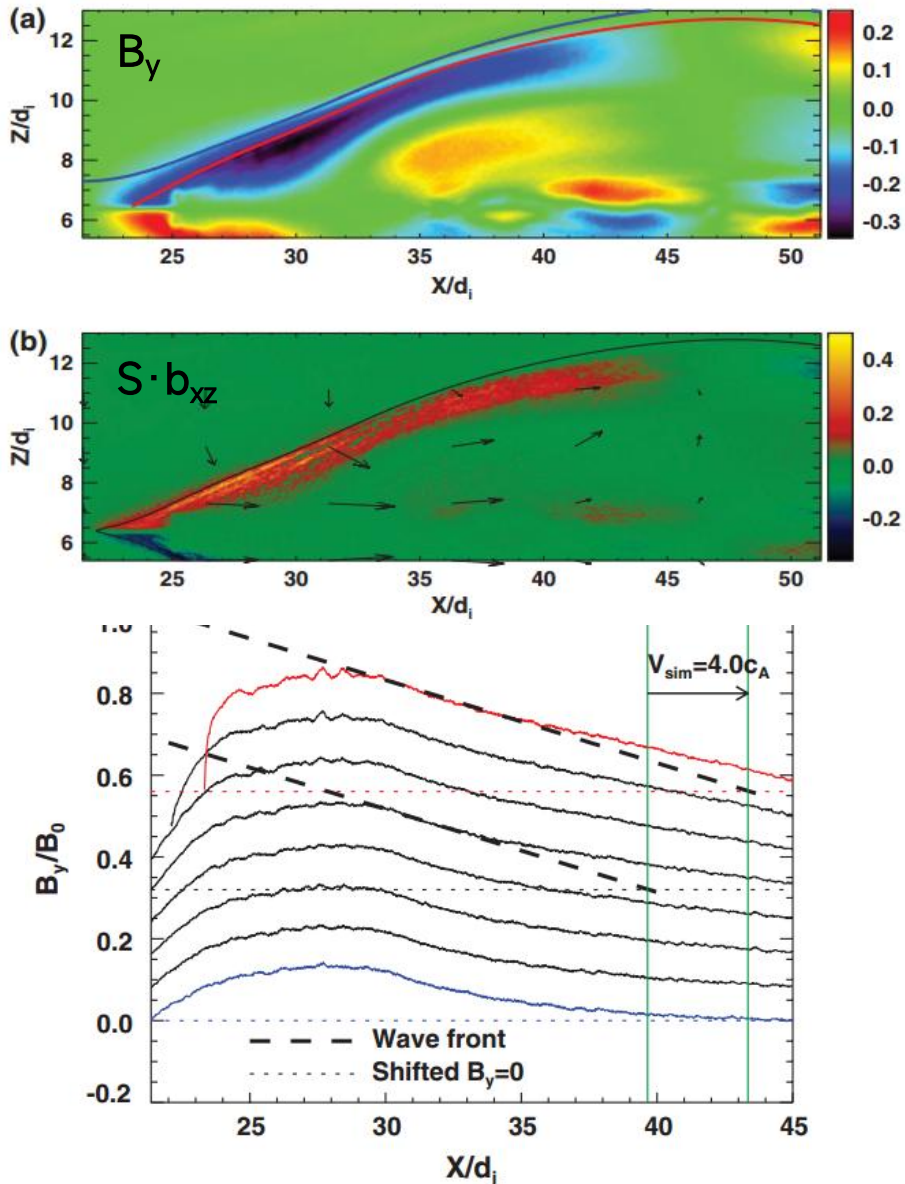
  在重联过程中产生的波和湍流会产生粒子扩散和异常电阻率，并加热、加速等离子体粒子，并影响磁重联过程。

Y. Ping, J. Zhong, X. Wang, B. Han, W. Sun, Y. Zhang, D. Yuan, C. Xing, J. Wang, and Z. Liu et al., Turbulent magnetic reconnection generated by intense lasers, Nat. Phys. 2023).
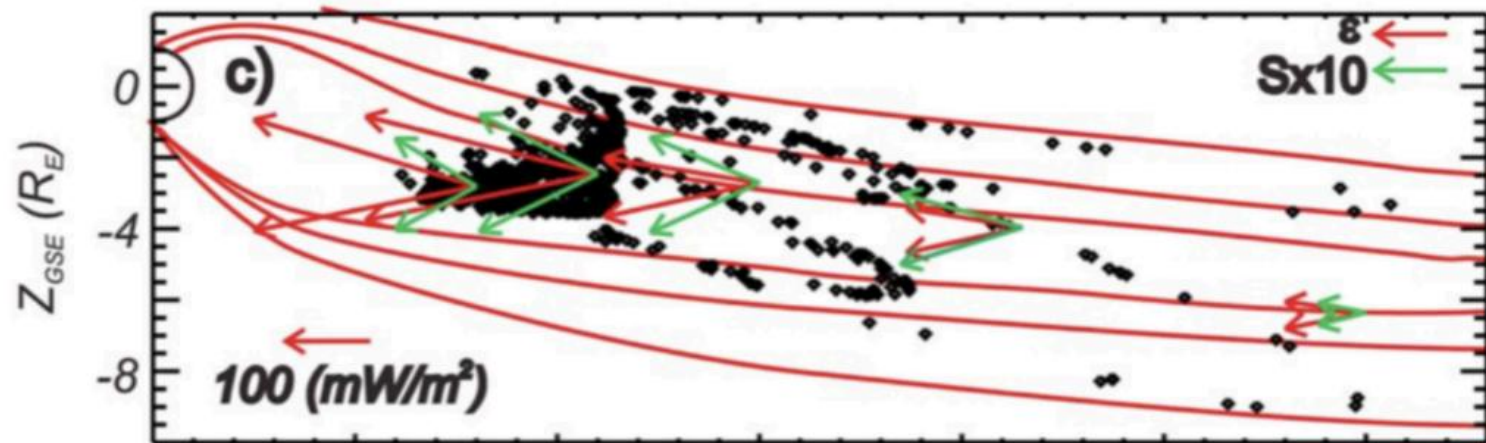
第一种哨声波位于重联下游的磁场堆积区，通过电子温度各向异性的激发形成，并沿着磁力线向下游传播；第二种哨声波位于分界线附近，通过电子束驱动的哨声不稳定性或电子洞非线性演化产生 Cerenkov 辐射，从而激发并向X线注入传播；
相较于以上两个区域扩散区内的哨声波发生率较低。

S.Y. Huang, Z.G. Yuan, F. Sahraoui, H.S. Fu, Y. Pang, M. Zhou, K. Fujimoto, X.H. Deng, A. Retinò, and D.D. Wang et al., Occurrence rate of whistler waves in the magnetotail reconnection region, J. Geophys Res. 122, 7188-7196 (2017).

磁重联与KAW

- B$_y$结构与separatrix平行，因此是具有k$_\parallel$‹‹k$_\perp$的强斜波（Alfvén waves and kinetic Alfvén waves）

- $\mathbf{B} = \hat{y} \times \nabla\varphi + B_y\hat{y}$，计算不同φ值下的KAW的B$_y$值，确定KAW的速度

- 对于磁尾参数，该波是超阿尔芬速度的（1500-5500 km/s），并产生大量坡印廷通量（10^{-5}-10^{-4}W/m^2)

M. Shay, J.F. Drake, J.P. Eastwood, and T.D. Phan, Super-Alfvénic propagation of substorm reconnection signatures and Poynting flux., Phys. Rev. Lett. 107 6, 65001 (2011).

磁重联与KAW

Average values of earthward ion energy flux (red arrows) and Poynting flux (green arrows) in the Earth's magnetotail

C.C. Chaston, J.W. Bonnell, L. Clausen, and V. Angelopoulos, Correction to "Energy transport by kinetic-scale electromagnetic waves in fast plasma sheet flows", J. Geophys Res. 117, (2012).
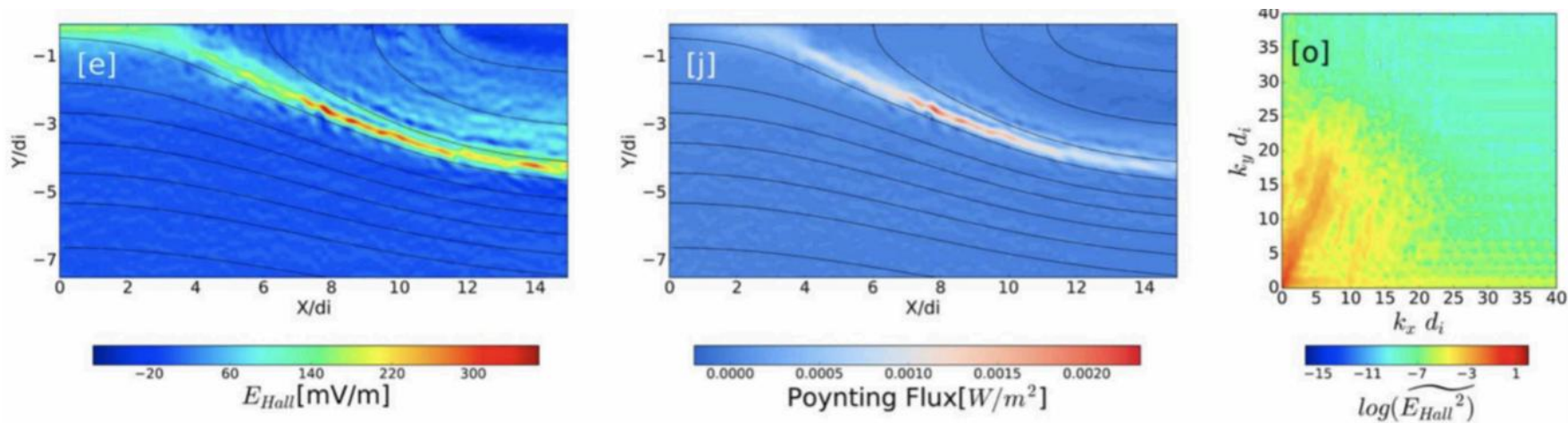
H. Huang, Y. Yu, L. Dai, and T. Wang, Kinetic Alfvén Waves Excited in Two-Dimensional Magnetic Reconnection, J. Geophys Res. 123, 6655-6669 (2018).

磁重联与KAW
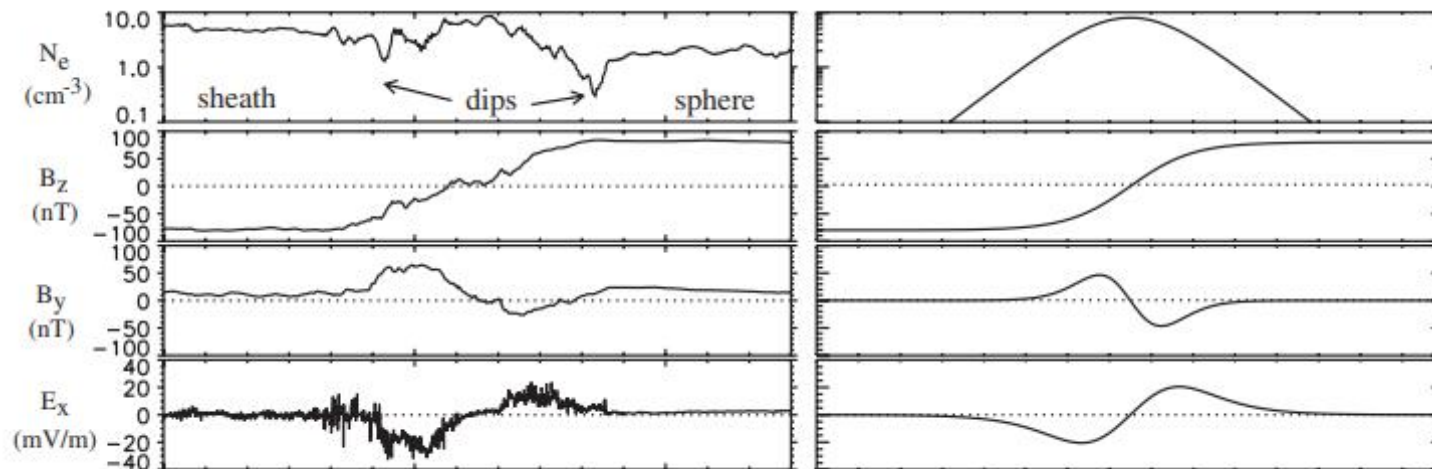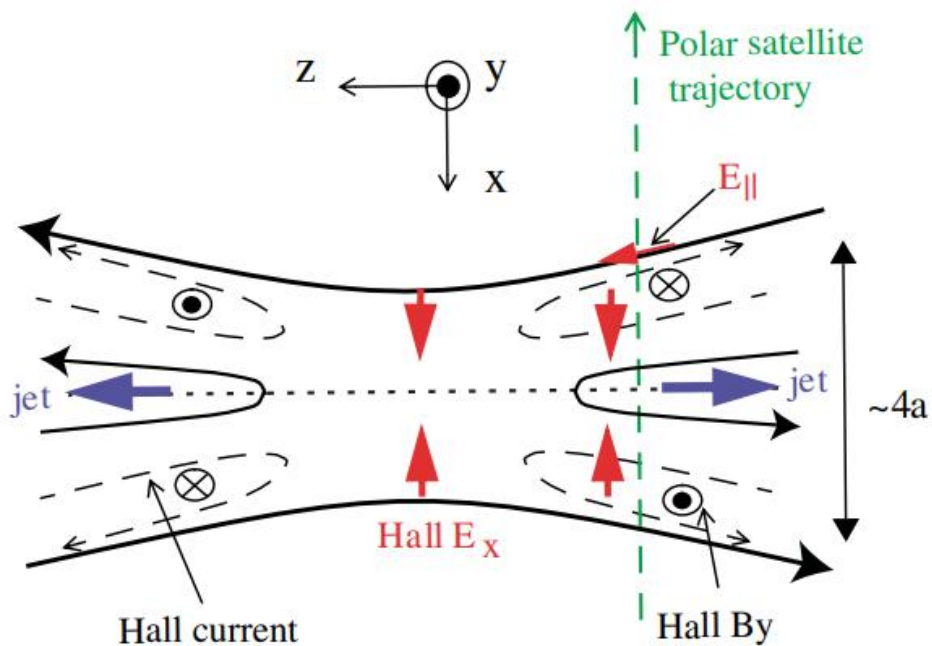
Polar观测结果与Harris sheet中n=1Alfven本征模理论预测结果的比较

Dai et al. 引入了四个KAW来描述无碰撞磁重联区域中的电磁场。这四个KAW形成了驻波，近似地可以被视为准稳定的波动结构。

作为磁场重联结构的一部分，KAW能够定量描述磁重联的电磁场和电流结构，包括霍尔磁场、霍尔电场、平行电场、霍尔电流、场向电流等，并导致较快的重联速率。

L. Dai, Collisionless Magnetic Reconnection via Alfve´n Eigenmodes, Phys. Rev. Lett. (2009).
L. Dai and C. Wang, Kinetic Alfven wave (KAW) eigenmode in magnetosphere magnetic reconnection, Reviews of Modern Plasma Physics 7, 2023).
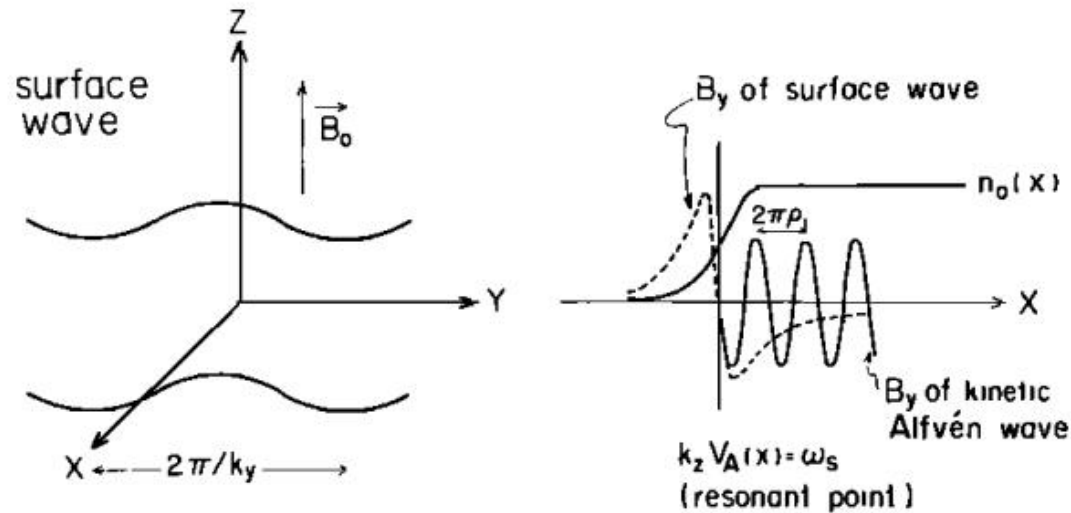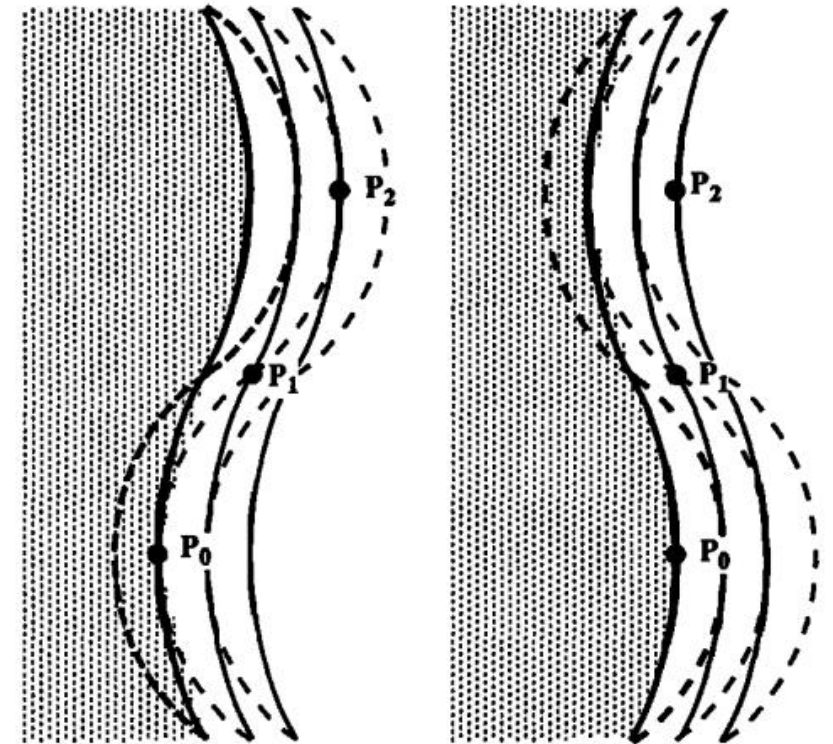
激光等离子体驱动磁重联中的KAW

KAW的激发：共振模式转化
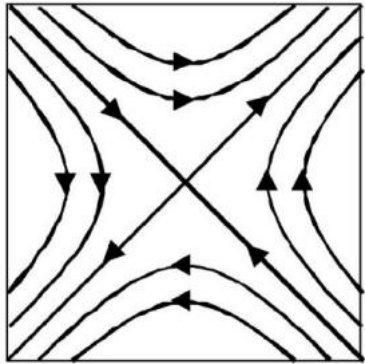
"X" type

MHD surface wave → KAW
This theory was first proposed by Hasegawa

A. Hasegawa, Particle acceleration by MHD surface wave and formation of aurora, J. Geophys. Res. 81, 5083 (1976).

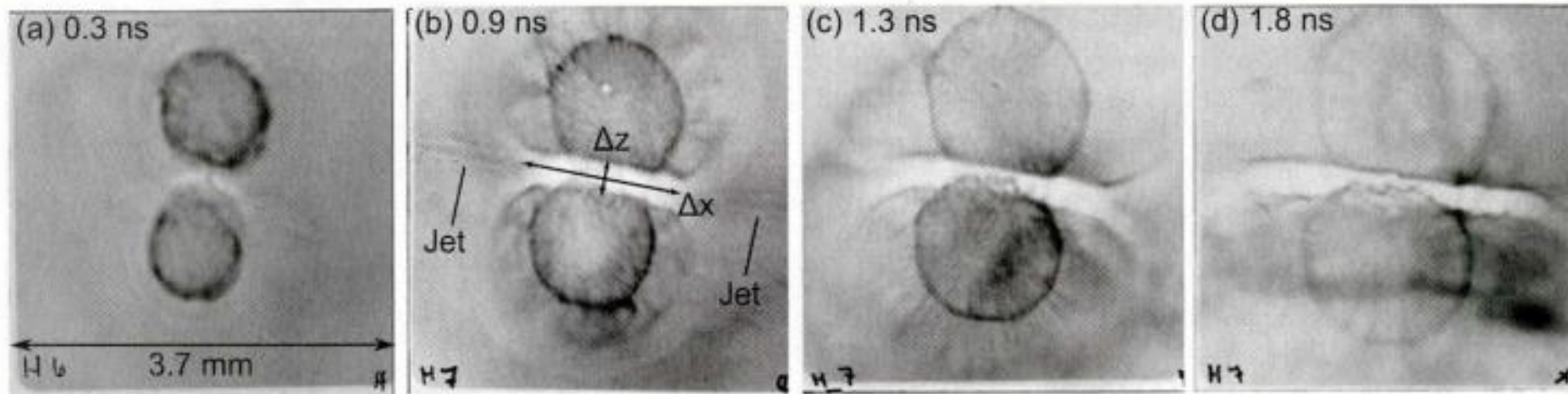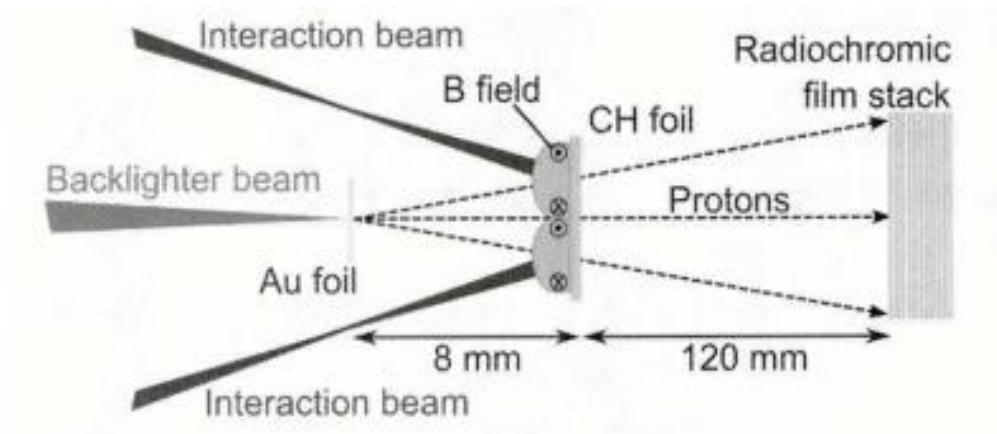- 不可压缩扰动
- 等离子体密度平滑变化
- KAW向高密度侧传播

KAW作用下离子跨磁力线传播

L.C. Lee, J.R. Johnson, and Z.W. Ma, Kinetic Alfvén waves as a source of plasma transport at the dayside magnetopause, J. Geophys. Res. 99, 17405 (1994).

激光等离子体驱动磁重联

M.J. Rosenberg et al. Slowing of Magnetic Reconnection Concurrent with Weakening Plasma Inflows……. Phys. Rev. Lett. 114, 205004 (2015).

激光等离子体驱动磁重联

P.M. Nilson, W. Fox, J. Matteucci, and D.H. Froula, A modified technique for laser-driven magnetic reconnection, LLE Review 158, 84 (2019).